The Elmore Delay as a Bound for RC Trees with Generalized Input Signals

Rohini Gupta, *Member, IEEE*, Bogdan Tutuianu, and Lawrence T. Pileggi, *Senior Member, IEEE*

***Abstract*—The Elmore delay is an extremely popular timing-performance metric which is used at all levels of electronic circuit design automation, particularly for resistor-capacitor (RC) tree analysis. The widespread usage of this metric is mainly attributable to it being a delay measure that is a simple analytical function of the circuit parameters. The only drawback to this delay metric is the uncertainty of its accuracy and the restriction to it being an estimate only for the step response delay.**

In this paper, we prove that the Elmore delay measure is an absolute upper bound on the actual 50% delay of an RC tree response. Moreover, we prove that this bound holds for input signals other than steps and that the actual delay asymptotically approaches the Elmore delay as the input signal rise time increases. A lower bound on the delay is also developed using the Elmore delay and the second moment of the impulse response. The utility of this bound is for understanding the accuracy and the limitations of the Elmore metric as we use it as a performance metric for design automation.

***Index Terms*—Delay estimation, Elmore delay (new), probability, RC trees (new).**

I. Introduction

RC TREES are commonly used to model digital logic gates and their associated interconnect paths at various stages of the design process. During the early phases of design, simple approximations or delay bounds are often applied since an exact solution of an approximate circuit model is superfluous.

The omnipresent Elmore delay [7], or first moment of the impulse response, is the delay approximation of choice for resistor-capacitor (RC) trees because of the ease with which it is calculated. In the original work of 1948, Elmore attempted to estimate the 50% delay of a monotonic step response by the mean of the impulse response. Penfield and Rubinstein [18] proved that RC tree step responses are indeed monotonic and thereby discovered the popular Elmore delay metric for analyzing gate and interconnect delays. However, because the median of the impulse response is the exact 50% delay and Elmore is approximating the median by the mean, Penfield and Rubinstein developed best and worst case bounds on the step response waveform [18].

These step response bounds were improved in [23] and later extended to a two-time constant approximation in [4]. Sometime later, higher order moment matching techniques were developed for resistor, inductor, capacitor (RLC) circuits [19], of which RC trees are an important subset. Higher order moments for RC trees can be calculated with excellent efficiency [22].

But even with the higher order approximations with accuracy comparable to SPICE, the Elmore delay remains a popular metric merely for its simplicity. It is used during logic synthesis to estimate wiring delays for approximate Steiner or spanning tree routes. It is used during performance driven placement and routing because it is the only delay metric which is easily measured in terms of net widths and lengths and so on. The only drawback to this delay metric is the uncertainty of its accuracy and the restriction to it being an estimate only for the step response delay.

In this paper we prove that the Elmore delay value is an absolute upper bound on the 50% delay of an RC tree. This is done by first proving that RC tree impulse response distributions are guaranteed to be unimodal and positively skewed. Then, using the classical theory of distribution functions, we show that the mean of such a distribution will always exceed the median. Moreover, we demonstrate that this proof applies not only to the step response, but also to any input forcing function which has a unimodal derivative, e.g., a saturated ramp with finite rise time. Finally, with a calculation of the mean and the variance of the impulse response we specify a lower bound on the 50% delay. We will show that the Elmore delay bound is sometimes better, sometimes worse, than the Penfield–Rubinstein 50% delay bound for the case of step inputs. In addition, we will show that the exact delay approaches the Elmore bound as the variance of the input-signal derivative increases.

II. RC Trees and Their Approximations

A. Interconnect Models

RC trees, such as the one shown in Fig. 1, have been widely used for modeling the gate and interconnect circuits like the one shown in Fig. 2. An RC tree is an RC circuit with capacitors from all nodes to ground, no capacitors between nonground nodes, and no resistors connected to ground, making it a natural model for characterizing digital gate and interconnect delays [18], [21]. For modeling simplicity, the

Manuscript received December 16, 1994; revised November 18, 1996. This work was supported in part by the Semiconductor Research Corporation under Contract 95-DJ-343 and the National Science Foundation under Contract MIP-9157263. This paper was recommended by Associate Editor, G. Zimmermann.

R. Gupta is with Bell Laboratories, Lucent Technologies, Allentown, PA 18103 USA.

B. Tutuianu is with Motorola Corp., Austin, TX 78758 USA.

L. T. Pileggi, formerly L. Pillage, is with the Department of Electrical and Computer Engineering, Carnegie Mellon University, Pittsburgh, PA 15213 USA.

Publisher Item Identifier S 0278-0070(97)02705-X.

0278–0070/97$10.00 © 1997 IEEE

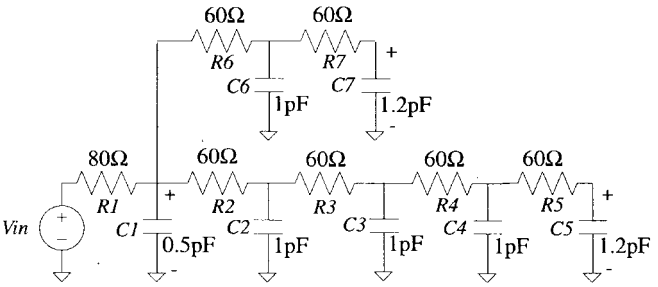

Fig. 1. A simple RC tree.

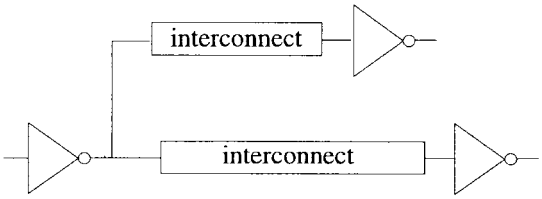

Fig. 2. A CMOS inverter driving a similar inverter through RC interconnect.

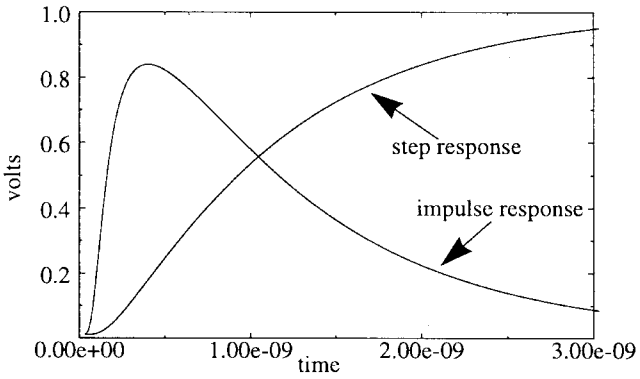

Fig. 3. The unit step and the unit impulse response (scaled by $1e+09$) for the voltage across C_5 in Fig. 1.

nonlinear driver in Fig. 2 is linearized as shown in Fig. 1. A great deal of work has been compiled over the last several years regarding these linearized gate models [1], [9], [10], [15], [16], [24]. In this work, however, we will focus on estimating the delay of the linearized RC tree in Fig. 1.

B. The Elmore Delay

The step response for the node voltage at capacitor C_5 of the RC tree in Fig. 1 is shown in Fig. 3. Also shown in Fig. 3 is the unit impulse response, $h(t)$, at the same node. Since the step response is the integral of the impulse response (transfer function), the 50% point delay of the monotonic step response (nonnegative transfer function) is the time τ at which

$$\int_0^\tau h(t)\,dt = 0.5. \tag{1}$$

Referring to Fig. 4, Elmore proposed to approximate τ by the mean of the $h(t)$ distribution.

Treating the nonnegative impulse response in Fig. 4 as a distribution function, the mean of this distribution function is defined by the first moment of the impulse response. Elmore's unit step response delay approximation, T_D, is

$$\begin{aligned} T_D &= m_1 \\ &= \int_0^\infty t h(t)\,dt \end{aligned} \tag{2}$$

when the area underneath $h(t)$ equals unity

$$\int_0^\infty h(t)\,dt = 1. \tag{3}$$

This approximation appears valid for the symmetrical function in Fig. 4, where the mean is equal to the median. However, it is somewhat erroneous for the real impulse response in Fig. 3, which is skewed asymmetrically. It is this skew, however, which will allow us to bound the delay (τ) by the mean (T_D) in this paper.

C. Calculating the Elmore Delay

The Elmore delay is a convenient metric for RC trees because it can be calculated so easily and efficiently for a particular circuit topology. Efficient path tracing algorithms for calculating the Elmore delay for RC trees have been covered extensively in the literature [18], [24], so they will not be discussed in detail here. In summary, one can calculate the Elmore delay from two $O(N)$ traversals of the tree, where N is the number of nodes in the tree. The Elmore value for the output at node i is given by

$$T_{D_i} = \sum_{k=1}^{N} R_{ki} C_k \tag{4}$$

where R_{ki} is the resistance of the portion of the (unique) path between the input and node i, that is common with the unique path between the input and node k, and C_k is the capacitance at node k [26]. Higher order moments can be obtained via path tracing with equal efficiency [19], [22]. The Elmore delay values at nodes C_1, C_5, and C_7 for the circuit in Fig. 1 are given in column (3) of Table I.

D. First Moment of the Impulse Response

The Elmore delay has also been used as a dominant time constant approximation. This follows from the transfer function for a response node of the RC tree expressed as

$$H(s) = \frac{1 + a_1 s + a_2 s^2 + \cdots + a_n s^n}{1 + b_1 s + b_2 s^2 + \cdots + b_m s^m} \tag{5}$$

where $m \geq n$. Expanding (5) about $s = 0$ yields $H(s)$ as an infinite series in powers of s

$$\begin{aligned} H(s) = 1 &+ (a_1 - b_1)s + (a_2 - b_2 - b_1 a_1 + b_1^2)s^2 \\ &+ (a_3 - b_3 - a_1 b_2 + 2 b_1 b_2 \\ &- a_2 b_1 + a_1 b_1^2 - b_1^3)s^3 + \cdots. \end{aligned} \tag{6}$$

The Laplace transform of $h(t)$ is

$$H(s) = \int_0^\infty h(t) e^{-st}\,dt. \tag{7}$$

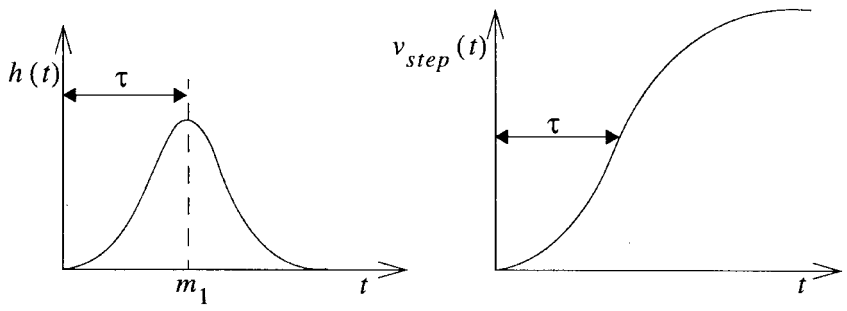

Fig. 4. Elmore's approximation.

TABLE I
DELAY BOUNDS FOR CIRCUIT IN FIG. 1

(1)	(2)	(3)	(4)	(5)	(6)	(7)
Node	**Actual delay**	**Elmore delay, T_D**	**Lower bound, $T_D - \sigma$**	**Single pole approx. $T_D \cdot \ln(2)$**	**PRH upper bound, t_{max}**	**PRH lower bound, t_{min}**
C1	0.196 ns	0.55 ns	0 ns	0.383 ns	0.55 ns	0 ns
C5	0.919 ns	1.2 ns	0.2 ns	0.83 ns	1.32 ns	0.51 ns
C7	0.45 ns	0.75 ns	0 ns	0.524 ns	1.02 ns	0.054 ns

Expanding e^{-st} about $s = 0$ in (7) yields the following series in powers of s

$$H(s) = \int_0^\infty h(t)\left[1 - st + \tfrac{1}{2}s^2t^2 - \tfrac{1}{6}s^3t^3 + \cdots\right] dt = \sum_{k=0}^{\infty} \frac{(-1)^k}{k!} s^k \int_0^\infty t^k h(t)\, dt. \tag{8}$$

From (8) we observe that the qth coefficient of the impulse response $h(t)$ is

$$m_q = \frac{(-1)^q}{q!} \int_0^\infty t^q h(t)\, dt. \tag{9}$$

These m_j's are related to the moments from distribution theory by the $(-1)^q/q!$ term. That is, the nth moment of a function $h(t)$ is defined to be $\int_0^\infty t^n h(t)\, dt$. It was this relation between moments and transfer function coefficients which led to Elmore's original work.

To understand the connection between the first moment and the dominant pole, we factor the numerator and the denominator of (5) and show that terms b_1 and a_1 are the sum of the reciprocal poles (circuit time constants) and the sum of the reciprocal zeros, respectively

$$b_1 = \sum_{j=1}^{m} \frac{1}{p_j}$$
$$a_1 = \sum_{j=1}^{n} \frac{1}{z_j}. \tag{10}$$

If there are no low-frequency zeros, the numerator coefficients, including a_1, are small and

$$T_D \cong b_1. \tag{11}$$

If one of the time constants (or poles) is dominant

$$\frac{1}{p_d} \gg \frac{1}{p_j}, \qquad j = 1, 2, \cdots, m, \quad j \neq d \tag{12}$$

then

$$T_D \cong \frac{1}{p_d}. \tag{13}$$

This dominant time constant approximation is then used to fit a single pole approximation

$$\nu(t) = 1 - e^{-p_d t}. \tag{14}$$

Solving (14) for the 50% point delay effectively scales the Elmore delay approximation by $\ln(2)$, or about 0.7.

We should point out that this dominant time constant delay prediction can be either pessimistic or optimistic at two different nodes in the same RC tree. For example, column (5) of Table I shows the values of $\ln(2) \cdot T_D$ at nodes C_1, C_5, and C_7 for the circuit in Fig. 1. Notice that, when compared with the actual delay values in column (1), the response at C_5 is optimistically predicted by $\ln(2) \cdot T_D$ while that at C_1 is pessimistically predicted. One way to explain this is by the excessive skew in the $h(t)$ distribution for C_1, which is shown with the step response for this node in Fig. 5, as compared with the skew for the response at C_5 (shown in Fig. 3). It can be expected that using $\ln(2) \cdot$ Mean to approximate the *median* will be vastly different for these two distributions.

It is difficult to know when a single pole dominates the low-frequency behavior of a circuit. For this reason, Rubinstein and Penfield established bounds for the step response delay of this important class of RC circuits.

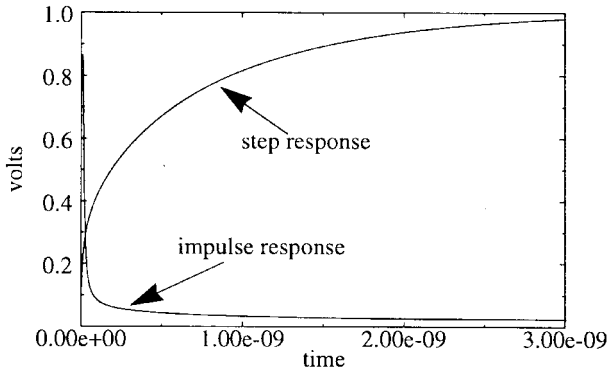

Fig. 5. The unit step and the unit impulse response (scaled by $4e+09$) for the voltage across C_1 in Fig. 1.

E. Penfield and Rubinstein's Bounds

Penfield and Rubinstein were the first to use the Elmore delay to analyze RC trees [18]. Before higher order moment matching techniques were available, delay bounds were the only means of estimating the accuracy of the RC tree delay approximation. The following are the Penfield–Rubinstein delay waveform bounds for any percentage point on the RC tree step response waveform

$$t_{\min}(\nu_i) = \begin{cases} 0, & 0 \le \nu_i \le 1 - \dfrac{T_{D_i}}{T_P} \\ T_{D_i} - T_P(1-\nu_i), & 1 - \dfrac{T_{D_i}}{T_P} \le \nu_i \le 1 - \dfrac{T_{R_i}}{T_P} \\ T_{D_i} - T_{R_i} + T_{R_i} \ln\left[\dfrac{T_{R_i}}{T_P(1-\nu_i)}\right], & 1 - \dfrac{T_{R_i}}{T_P} \le \nu_i < 1 \end{cases}$$

$$t_{\max}(\nu_i) = \begin{cases} \dfrac{T_{D_i}}{1-\nu_i} - T_{R_i}, & 0 \le \nu_i \le 1 - \dfrac{T_{D_i}}{T_P} \\ T_P - T_{R_i} + T_P \ln\left[\dfrac{T_{D_i}}{T_P(1-\nu_i)}\right], & 1 - \dfrac{T_{D_i}}{T_P} \le \nu_i < 1 \end{cases} \tag{15}$$

where

$$T_P = \sum_k R_{kk} C_k,$$

$$T_{D_i} = \sum_k R_{ki} C_k,$$

$$T_{R_i} = \frac{\sum_k R_{ki}^2 C_k}{R_{ii}}. \tag{16}$$

Calculating these bounds requires calculating two additional terms in addition to the Elmore delay. All of these terms, however, are obtained with $O(N)$ complexity. The values of $t_{\max}$ and $t_{\min}$ at the 50% point for our example in Fig. 1 are given in columns (6) and (7) of Table I. Note that $t_{\max} > T_D$ at the loads, C_5 and C_7, and $t_{\max} = T_D$ at the driving point, C_1. Also note the values of $t_{\min}$ as a lower bound on the delay.

In general, one can also calculate more moments for the RC tree, and generate a two-pole [4] or a q-pole [19] approximation. Higher order moments are obtained with $O(N)$ complexity too. But for certain applications, a single term delay metric, such as the Elmore expression, is invaluable, and this paper is towards a better understanding of this approximation.

III. The Elmore Delay as a Bound

Referring back to Figs. 3 and 5, it is apparent that with such an asymmetrical distribution for the impulse response, the mean would not coincide with the median. In this section, we will show that these asymmetric distributions have a "long tail" on the right side of the mode, which is roughly the maximum value point, and a "short tail" on the left side. Such distributions are said to have *positive* skew. We will also prove that the impulse response for an RC tree is unimodal and then use these two properties to prove that

$$\text{Mode} \le \text{ Median} \le \text{ Mean}. \tag{17}$$

Equation (17) states that the Elmore delay, or the mean of the impulse response, is truly an upper bound on the median, or the 50% point delay. We will show that this holds for any input that has a unimodal derivative and that the mean becomes a better approximation of the median as the rise time of the input-signal increases. Further in the section, we will also provide a lower bound on the 50% delay for an RC tree, but first a few definitions.

Definition 1: The mode, M, of a distribution function is that value of the variate exhibited by the greatest number of members of the distribution [11]. If the distribution function is continuous and differentiable, a unique mode exists only if f is unimodal and is the solution of

$$f'(x) = \frac{d}{dx} f(x) = 0$$
$$f''(x) = \frac{d^2}{dx} f(x) < 0. \tag{18}$$

Definition 2: The *median* m of a distribution function f is that value of the variate which divides the total frequency into two equal halves [11], i.e.,

$$\int_{-\infty}^{m} f(x)\,dx = \int_{m}^{\infty} f(x)\,dx = \tfrac{1}{2}. \tag{19}$$

Definition 3: The *mean* μ of a distribution function f about the point $x = a$ is defined by

$$\mu = \int_{-\infty}^{\infty} (x-a) f(x)\,dx. \tag{20}$$

Definition 4: A density function $h(t)$ is called *unimodal*, if and only if, there exists at least one value $t = t_m$ such that $h(t)$ is nondecreasing for $t < t_m$ and nonincreasing for $t > t_m$ [20].

Definition 5: Coefficient of skewness for a distribution function is given by $\gamma = \mu_3/\sigma^3$, where $\sigma = \sqrt{\mu_2}$, and μ_2 and μ_3 are the second and third central moments of the distribution function, respectively [5].

Lemma 1: The impulse response $h(t)$ at any node of an RC tree is a unimodal and positive function.

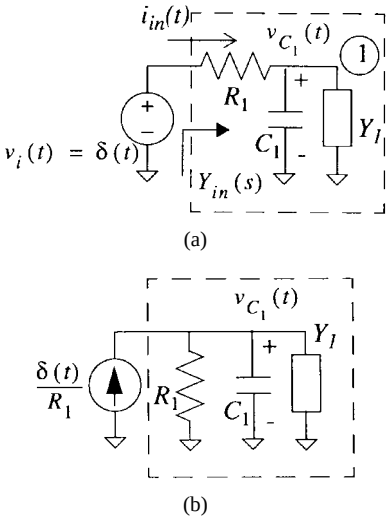

Fig. 6. (a) Input node of an RC tree with input admittance $Y_{in}(s)$. (b) Norton equivalent for the circuit in Fig. 6(a).

Proof: The proof is by induction. For a general RC circuit as shown in Fig. 6(a), if $\nu_i(t)$ is a unit impulse input, from the Norton equivalent circuit shown in Fig. 6(b), the effect of the unit impulse is to charge the capacitor C_1so that

$$\nu_{C_1}(0+) = \frac{1}{C_1}\int_{0-}^{0+} \frac{\delta(t)}{R_1}\,dt = \frac{1}{R_1C_1}. \tag{21}$$

Since $\nu_i(t)$ is an impulse input, for $t > 0$, $\nu_i(t) = 0$ in Fig. 6(a). The impulse response at node one is then given by the voltage $\nu_{C_1}(t)$ at the discharging capacitance C_1 after the initial state has been established by the impulse input $\delta(t)$. For a general RC circuit, the poles and zeros of the driving point admittance, $Y_{in}(s)$ in Fig. 6(a) are simple, interlaced, and are located on the negative real axis of the s plane [25]. Furthermore, the residues at the poles of $Y_{in}(s)$ are real and negative [25]. In Fig. 6(a), for $t > 0$, the natural response is given by the poles of $Y_{in}(s)$ [8] and is therefore of the form

$$i_{in}(t) = \alpha\left[\sum_i (-k_i)e^{-p_i t}\right], \qquad k_i > 0, \quad p_i > 0 \tag{22}$$

where p_i and k_i are the poles and residues of $Y_{in}(s)$, respectively, and $\alpha > 0$ is a constant to satisfy the initial condition, $\nu_{C_1}(0+)$, so that $\alpha(\sum_i k_i)R_1 = 1/R_1C_1$. From KCL, $\nu_{C_1}(t) = \nu_i(t) - i_{in}(t)R_1$, so that the impulse response at node one is given by

$$h_1(t) = -i_{in}(t)R_1 = \alpha\left(\sum_i k_i e^{-p_i t}\right)R_1. \tag{23}$$

Following Definition 4, $h_1(t)$ is unimodal.

Now consider Fig. 7 which shows node k and the RC tree "downstream" from node k. For the induction argument, assume that $h_k(t)$ is unimodal, and

$$\nu_{k+1}(t) = \nu_k(t) - R_k i_{k,\,k+1}(t). \tag{24}$$

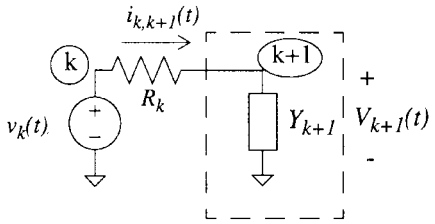

Fig. 7. Admittance Y_{k+1} of an RC tree at an arbitrary node $k+1$.

If $\nu_k(t)$ is an impulse input at node k, then $h_{k,\,k+1}(t)$ is the impulse response at node $k+1$ for the tree rooted at node k. This has the same form as in (23) and is unimodal. Thus, the impulse response at node $k+1$ w.r.t. node one (the driving point), $h_{k+1}(t)$, is given by

$$h_{k+1}(t) = h_{k,\,k+1}(t) * h_k(t) \tag{25}$$

where * is the convolution operator. Since the convolution of two unimodal positive functions is also a unimodal function [20], $h_{k+1}(t)$ is unimodal. Thus, $h(t)$ at any node of an RC tree is a unimodal function. That $h(t)$ is a positive function has been shown in [23]. □

Lemma 2: For the impulse response $h(t)$ at any node of an RC tree, the coefficient of skewness γ is always nonnegative.

Proof: The proof again follows an induction-based argument. Following Definition 5, it needs to be shown that for $h(t)$ at any node of an RC tree, $\mu_3 \geq 0$ and $\mu_2 \geq 0$. In this proof, it is first shown that the coefficient of skewness γ is positive at the first node of an RC tree, and then the additive property of *central moments* over convolution (Appendix B) is used to motivate the induction argument.

In Fig. 8(a), consider a general RC tree for which the first three moments of the driving point admittance, $Y_1(s)$ at node one, can be used to synthesize a π-model as shown in Fig. 8(b) [14]. Note that this π model exactly matches the first three moments of the driving point admittance of the original RC circuit. In terms of the moments of $Y_1(s)$, the π-model parameters are

$$\begin{aligned} R_2 &= -\frac{[m_3(Y_1)]^2}{[m_2(Y_1)]^3} \\ C_1 &= m_1(Y_1) - \frac{[m_2(Y_1)]^2}{m_3(Y_1)} \\ C_2 &= \frac{[m_2(Y_1)]^2}{m_3(Y_1)} \end{aligned} \tag{26}$$

where $m_1(Y_1)$, $m_2(Y_1)$, $m_3(Y_1)$ are the first three moments of $Y_1(s)$.

With $m_0 = 1$, the central moments μ_2 and μ_3 of the transfer function $H_1(s)$ at node one can be expressed in terms of the moments m_k as

$$\mu_2 = 2m_2 - m_1^2$$

and

$$\mu_3 = -6m_3 + 6m_1m_2 - 2m_1^3. \tag{27}$$

It is shown in Appendix A that the moments $m_0(H_1)$ through $m_3(H_1)$ of the transfer function $H_1(s)$ at node one in Fig. 8(a)

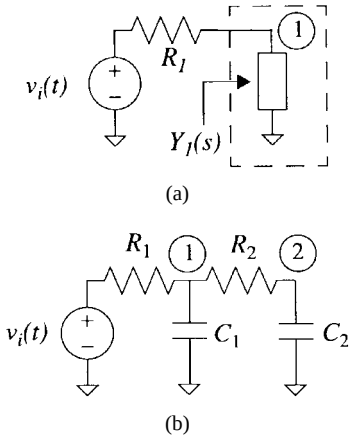

Fig. 8. (a) Driving point admittance of an RC tree at the first capacitor node. (b) A reduced order π model for the $Y_1(s)$ in (a).

are a function only of the moments $m_0(Y_1)$ through $m_3(Y_1)$ of the driving point admittance $Y_1(s)$. Therefore, an analysis of the π model in Fig. 8(b) provides the exact values of the coefficients $m_0(H_1)$ through $m_3(H_1)$ of the transfer function $H_1(s)$.

For the RC circuit in Fig. 8(b) (Appendix B)

$$\begin{aligned}\mu_2^{(1)} &= 2m_2^{(1)} - [m_1^{(1)}]^2 \\ &= R_1^2(C_1^2 + C_2^2) + 2R_1^2C_1C_2 + 2R_1R_2C_2^2 \\ &\geq 0 \end{aligned} \tag{28}$$

$$\begin{aligned}\mu_3^{(1)} &= -6m_3^{(1)} + 6m_1^{(1)}m_2^{(1)} - 2[m_1^{(1)}]^3 \\ &= 6R_1R_2C_2^2[R_1(C_1 + C_2) + R_2C_2)] + 2[R_1(C_1 + C_2)]^3 \\ &\geq 0 \end{aligned} \tag{29}$$

where $m_k^{(1)}$ denotes the kth moment of the transfer function at node one. Thus, for the impulse response $h_1(t)$ at node one in Fig. 8(b), from (28) and (29) and Definition 2, $\gamma \geq 0$.

Next consider Fig. 9 which shows node k and its "downstream" part of the RC tree. To complete the induction argument, assume that at node k, $\mu_3 \geq 0$ and $\mu_2 \geq 0$ for $h_k(t)$, and hence, $\gamma \geq 0$. If $\nu_k(t)$ is an impulse, then $h_{k,\,k+1}(t)$ is the impulse response at node $k+1$ w.r.t. the input at node k. This has the same form as in Fig. 8(a) for which the above argument shows that $\mu_3 \geq 0$ and $\mu_2 \geq 0$ from (28) and (29). Now, the impulse response at node $k+1$ w.r.t. node one, $h_{k+1}(t)$, is given by

$$h_{k+1}(t) = h_{k,\,k+1}(t)^* h_k(t). \tag{30}$$

When $m_0 = 1$, the second and third central moments add under convolution (Appendix B). Thus

$$\begin{aligned}\mu_2(h_{k+1}) &= \mu_2(h_{k,\,k+1}) + \mu_2(h_k) \geq 0 \\ \mu_3(h_{k+1}) &= \mu_3(h_{k,\,k+1}) + \mu_3(h_k) \geq 0. \end{aligned} \tag{31}$$

Thus, for $h_{k+1}(t)$, from Definition 5, $\gamma \geq 0$. Thus, for every node in an RC tree, the *coefficient of skewness*, $\gamma \geq 0$. □

Theorem: For the impulse response $h(t)$ at any node in an RC tree

$$\text{Mode} \leq \text{ Median} \leq \text{ Mean}. \tag{32}$$

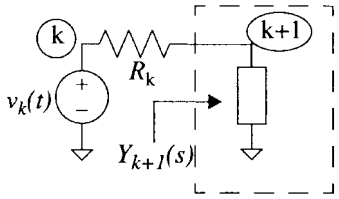

Fig. 9. Admittance Y_{k+1} of an RC tree at an arbitrary node $k+1$.

Proof: For a unimodal "skewed" distribution function, the mean, median, mode inequality states that these three quantities occur either in alphabetical order or the reverse alphabetical order [11], i.e., either Mean $\leq$ Median $\leq$ Mode or Mode $\leq$ Median $\leq$ Mean. From Lemmas 1 and 2, we have that each node in an RC tree has a unimodal distribution function for which $\gamma \geq 0$. We now prove, by contradiction, that for an RC tree we have that Mode $\leq$ Median $\leq$ Mean.

For our contradiction argument, let Mean $\leq$ Median $\leq$ Mode hold for any node, α, in an RC tree. In a symmetrical distribution, for which the coefficient of skewness, γ, is exactly zero, the mean, the median and the mode coincide [11], [13]. Thus a natural measure of skewness for an asymmetrical distribution is the deviation of the *mean* from the *median*, or the *mean* from the *mode*. Thus

$$\text{Skew} = \frac{\text{Mean} - \text{ Median}}{\sigma} \tag{33}$$

where $\sigma = \sqrt{\mu_2}$. Thus, at the node α, since Mean $\leq$ Median $\leq$ Mode holds, skew is negative. But, from Lemma 2, we have that the coefficient of skewness, $\gamma \geq 0$. Thus, at α, either Skew $= 0$ or we have a contradiction. In the former case, Mean $=$ Median $=$ Mode, i.e., the distribution is symmetric, and the mean and median coincide. And in the latter case, Mode $\leq$ Median $\leq$ Mean.

Since the choice of the node α is arbitrary, the proof is complete. □

We should note at this point that the Elmore delay T_D or the mean μ of the impulse response approaches the 50% delay point at nodes further downstream from the source in an RC tree. Thus, as one moves away from the source, μ is a better approximation of the net delay, as further discussed in Section IV.

A. A Lower Bound on Delay

Corollary 1: A lower bound on the 50% delay for an RC tree is given by

$$\max(\mu - \sigma, 0) \tag{34}$$

where μ is the mean and $\sigma = \sqrt{\mu_2}$.

Proof: Consider an impulse response $h(t)$, shown in Fig. 10, with mean at $t = \mu$. We define another function $H(t)$ as

$$H(t) = \int_{-\infty}^{t} h(\zeta)\, d\zeta. \tag{35}$$

With a simple change in the x coordinate such that $\tau = t - \mu$, we have $h(\tau)$ such that its mean is at $\tau = 0$ in the new

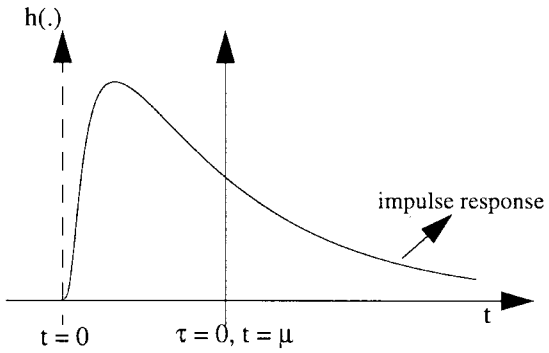

Fig. 10. Impulse response $h(t)$ at an arbitrary node of an RC tree.

coordinate system. Then, we use the following inequality from [5, p. 256]

$$H(\tau) \leq \frac{\sigma^2}{\sigma^2+\tau^2}, \qquad \tau < 0. \tag{36}$$

For $\tau = -\sigma$, (35) and (36) show that

$$\begin{aligned} H(-\sigma) &= \int_{-\infty}^{-\sigma} h(\zeta)\, d\zeta \\ &\leq \frac{\sigma^2}{\sigma^2+(-\sigma)^2} \\ &= \tfrac{1}{2}. \end{aligned} \tag{37}$$

Equation (37) states that in the new coordinate system, $\tau = -\sigma$ is less than the median. Thus, in the original coordinate system, for $h(t)$ we have that $\mu - \sigma \leq$ Median.

When $\mu \leq \sigma$, since the RC tree system is causal and relaxed [3] with zero input for $t < 0$, we have Median ≥ 0, and hence $\mu - \sigma \leq 0 \leq$ Median. This completes the proof. □

Referring back to the example in Fig. 1 and the delay bounds in Table I, the $\mu - \sigma$ lower bound at C_1 equals $t_{\min}$, whereas at C_5 and C_7, $t_{\min}$ is a tighter lower bound than $\mu - \sigma$. However, as observed in Section III, the Elmore delay upper bound, μ, becomes a tighter upper bound at the leaf-nodes of an RC tree as is evident at C_5 and C_7 in Table I.

B. Approximating the Output Signal Transition Time

Another measure of practical importance for RC circuits, other than the 50% delay point, is the rise time, T_R, which may be defined as the time required for the response to increase from 10%–90% of its final value [7]. A good measure of the value of T_R for an output response is

$$T_R \propto \sigma = \sqrt{\mu_2} \tag{38}$$

where μ_2 is the second central moment of the output response. Elmore also proposes this value, which he calls the *radius of gyration*, as a rise time measure for step-responses [7].

IV. General Input Signals

The above shows that the Elmore delay is an upper bound on the 50% step response delay. In addition, with one more moment the variance can be calculated to establish a lower bound on the 50% delay. However, when using the Elmore delay to estimate RC interconnect delays, the signal coming out of the digital gate is never a step voltage and is generally modeled by a saturated ramp. Of course several models have been developed to characterize the switching gate by a linear resistor and a voltage step for compatibility with the Elmore-step-response model [1], [9], [10], [16], [24] but at the expense of accuracy. One recent work attempts to model high-speed CMOS gates with linear resistors for efficiency, but time varying voltage sources to capture the high-frequency phenomena such as resistance shielding and effective capacitance [6]. Most timing analyzers characterize the gate and output signal transition time empirically as a function of load and then drive the RC tree interconnect model with a voltage that represents this transition time. For these reasons we extend this Elmore-based bound to consider nonzero input signal transition time, or more appropriately, the variance of the input signal's derivative.

A. The Elmore Delay Upper Bound

Corollary 2: For an RC circuit with a monotonically increasing, piecewise-smooth input $\nu_i(t)$ such that $\nu_i'(t)$ is a unimodal function, Mode $\leq$ Median $\leq$ Mean holds for the output response $\nu_0(t)$ at any node.

Proof: The output response $\nu_0(t)$ at any node of an RC tree in response to an input $\nu_i(t)$ is given in the Laplace domain by

$$V_o(s) = H(s) \cdot V_i(s) \tag{39}$$

where $H(s)$ is the transfer function of the circuit at that node. Also, $\nu_i(t)$ is a piecewise-smooth function and hence piecewise differentiable. Thus

$$\begin{aligned} \mathcal{L}\{\nu_o'(t)\} &= s\mathcal{L}\{\nu_o(t)\} - \nu_o(0) \\ &= s\mathcal{L}\{h(t)^*\nu_i(t)\} \qquad \text{since } \nu_o(0) = 0 \\ &= \mathcal{L}\{h(t)\}\mathcal{L}\{\nu_i'(t)\} \qquad \text{since } \nu_i(0) = 0 \end{aligned} \tag{40}$$

where $\mathcal{L}(\,.\,)$ is the Laplace transform operator. Further, from Appendix B, we have the property that the second and third central moments add under convolution. Thus

$$\begin{aligned} \mu_2[\nu_o'(t)] &= \mu_2[h(t)] + \mu_2[\nu_i'(t)] \\ \mu_3[\nu_o'(t)] &= \mu_3[h(t)] + \mu_3[\nu_i'(t)]. \end{aligned} \tag{41}$$

From Lemma 2, we know that $\mu_2[h(t)] \geq 0$ and $\mu_3[h(t)] \geq 0$. From hypothesis, we also have

$$\begin{aligned} \mu_2[\nu_i'(t)] &\geq 0 \\ \mu_3[\nu_i'(t)] &\geq 0. \end{aligned} \tag{42}$$

From (41) and (42), therefore, $\mu_2[\nu_o'(t)] \geq 0$ and $\mu_3[\nu_o'(t)] \geq 0$. Thus, from Definition 5, $\gamma[\nu_o'(t)] \geq 0$, and Median $\leq$ Mean. □

Corollary 3: For a finite sized RC circuit with a monotonically increasing piecewise-smooth input $\nu_i(t)$ such that $\nu_i'(t)$ is a symmetric function, as the rise time of the input signal, $t_r \to \infty$, the 50% delay of the output response $\to T_D$, i.e., Median $\to$ Mean.

Proof: The output response $\nu_o(t)$ at any node of an RC tree in response to an input $\nu_i(t)$ is given in the Laplace domain by

$$V_o(s) = H(s) \cdot V_i(s). \tag{43}$$

And from (40) and (41)

$$\begin{aligned} \mu_2[\nu_o'(t)] &= \mu_2[h(t)] + \mu_2[\nu_i'(t)] \\ \mu_3[\nu_o'(t)] &= \mu_3[h(t)] + \mu_3[\nu_i'(t)]. \end{aligned} \tag{44}$$

From hypothesis, we have that $\nu_i'(t)$ is a symmetric function. $\therefore \mu_3[\nu_i'(t)] = 0$. Also, since $\mu_2[\nu_i'(t)] \propto t_r$

$$t_r \to \infty \Rightarrow \mu_2[\nu_i'(t)] \to \infty. \tag{45}$$

Also from hypothesis, the circuit is finite sized. $\therefore |\mu_3[h(t)]| < \infty$. Thus

$$\gamma[\nu_o'(t)] = \frac{\mu_3[\nu_o'(t)]}{\{\mu_2[\nu_o'(t)]\}^{3/2}} \to 0 \qquad \text{as } t_r \to \infty. \tag{46}$$

Since $\gamma \propto$ Mean $-$ Median, $\gamma \to 0 \Rightarrow$ Median $\to$ Mean. Thus, as the rise time of the input-signal increases without bound, the 50% delay for an RC tree approaches the Elmore delay T_D. □

It is noteworthy here that since $\mu_3[\nu_i'(t)] = 0$, i.e., $\nu_i'(t)$, is a symmetric function, its mean and median coincide. Further

$$\begin{aligned} &\mu[\nu_o'(t)] - \mu[\nu_i'(t)] = T_D \\ \Rightarrow &\int_0^\infty t\nu_o'(t)\,dt - \int_0^\infty t\nu_i'(t)\,dt = T_D \end{aligned} \tag{47}$$

where $\mu(.)$ is the *mean*. Integrating by parts

$$\begin{aligned} &\Rightarrow \left\{ \int_0^\infty [1-\nu_o(t)]\,dt - t[1-\nu_o(t)]\Big|_0^\infty \right\} \\ &\quad - \left\{ \int_0^\infty [1-\nu_i(t)]\,dt - t[1-\nu_i(t)]\Big|_0^\infty \right\} = T_D \\ &\Rightarrow \int_0^\infty [1-\nu_o(t)]\,dt - \int_0^\infty [1-\nu_i(t)]\,dt = T_D \end{aligned} \tag{48}$$

where we have used the fact that $\lim_{t\to\infty} t[1-\nu_o(t)] = 0$ and $\lim_{t\to\infty} t[1-\nu_i(t)] = 0$ since both $\nu_o(t)$ and $\nu_i(t) \to 1V$ exponentially as $t \to \infty$ [26]. Thus, (48) says that the area between the input and the output response equals the Elmore Delay, T_D [12].

B. Delay Curves

The estimation of the 50% delay by the Elmore delay as a function of the rise time of the input signal (see Fig. 11), as stated in Corollary 3, is shown in Fig. 12 for our RC tree example circuit (in Fig. 1). As the rise time of the input signal increases, the delay asymptotically approaches the Elmore Delay value, T_D (from below), as expected.

It was observed in Section III that as one moves away from the source, T_D (i.e., the mean, η) is a better approximation of the net delay. The proof for Lemma 1 uses the additive property of the central moments under convolution. Referring to (31), for any node k, $\mu_2(h_k)$, $\mu_3(h_k) \geq 0$. Furthermore, using (28) and (29), it is clear that since R_2, C_1, and C_2 decrease as one moves further from the driving point, $\mu_2(h_{k,k+1})$ and $\mu_3(h_{k,k+1})$ form decreasing and hence convergent sequences. Thus, as nodes farther away from the source are considered, the values of $\mu_2(h_k)$ and $\mu_3(h_k)$ start to converge and hence the skew, γ, converges. The fact that T_D is a better approximation of the net delay farther away from the driving point is illustrated here using a 25-node RC tree. For three nodes A, B, and C, where A is near the driving point, B is in the middle of the tree, and C is a leaf-node, the impulse responses are shown in Fig. 13. The response at node C is less "asymmetric" than the response at node B, which shows that the impulse response approaches symmetry away from the driving point and the Elmore delay T_D becomes a tighter bound on the 50% delay point.

Table II shows the relative errors (Delay $- T_D$)/Delay for different input signal rise times. In Fig. 14, the relative error decreases as a function of the distance from the driving point and input signal rise time.

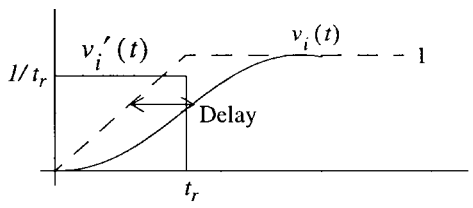

Fig. 11. Input signal $\nu_i(t)$ with rise time, t_r, and its derivative, $\nu_i'(t)$.

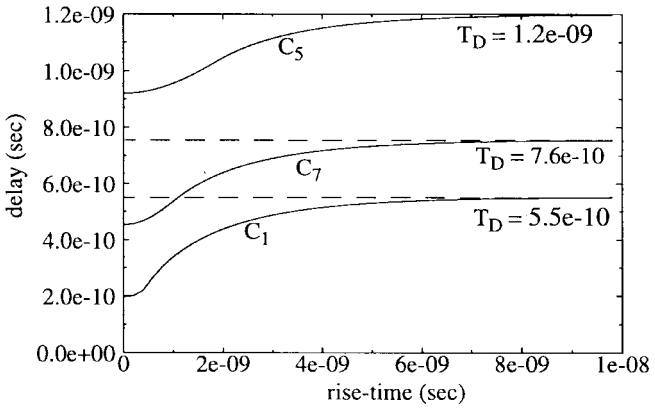

Fig. 12. Delay curves show that as the rise time of the input signal increases, the delay approaches T_D.

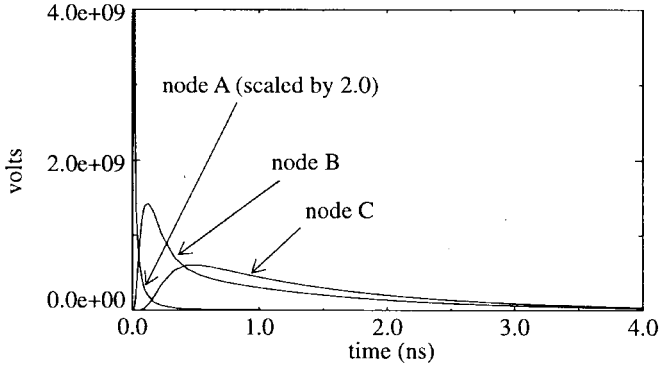

Fig. 13. Impulse responses at nodes A (driving point), B (middle node), and C (leaf node).

TABLE II
DELAYS AND RELATIVE ERROR AT NODES A, B, C ALONG A SIGNAL PATH

Node	Elmore delay	Rise-time = 1ns		Rise-time = 5ns		Rise-time =10ns	
		Delay	% Error	Delay	% Error	Delay	% Error
A	0.02 ns	0.01 ns	104%	18.0 ps	11.9%	19.0 ps	1.54%
B	1.13 ns	0.72 ns	54.7%	1.06 ns	6.5%	1.116 ns	0.86%
C	1.56 ns	1.2 ns	29.6%	1.48 ns	4.8%	1.547 ns	0.64%

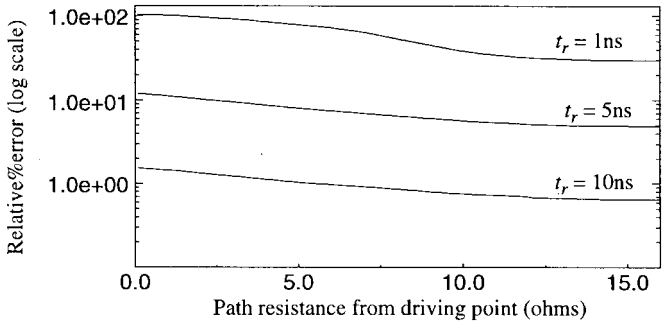

Fig. 14. Relative error (Delay $- T_D$)/Delay as function of path resistance from driving point (i.e., distance from driving point).

V. CONCLUSIONS

The Elmore delay is an extremely popular timing performance metric which is used at all levels of electronic circuit design automation. We have proven that this delay measure is an upper bound on the actual 50% delay of an RC tree response. Moreover, we have proven that this bound holds for input signals other than steps and that the actual delay asymptotically approaches the Elmore delay as the input signal rise time increases. A lower bound on the delay is also developed as a function of the Elmore delay, which is the first moment of the impulse response, along with the second moment of the impulse response. Improved bounds may be possible with more moments, but moment matching techniques, such as asymptotic waveform evaluation (AWE), are preferable when higher order moments are available. The utility of this bound is for understanding the accuracy and the limitations of the Elmore metric as we use it as a performance metric.

APPENDIX A
DRIVING POINT ADMITTANCE IN LEMMA 2

With reference to Fig. 15, the transfer function at node one is given by

$$H_1(s) = \frac{\dfrac{1}{Y_1(s)}}{R_1 + \dfrac{1}{Y_1(s)}} = \frac{1}{R_1 Y_1(s) + 1}. \tag{A1}$$

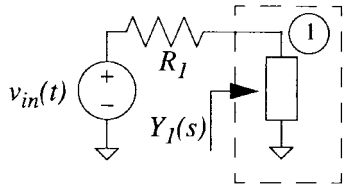

Fig. 15. Moments of the transfer function $H_1(s)$ at node one as a function of the driving point admittance $Y_1(s)$ of the RC tree at node one.

If $m_k(Y_1)$ is the kth moment of the driving point admittance $Y_1(s)$ of the RC circuit, then $Y_1(s)$ can be rewritten as a series

$$Y_1(s) = m_0(Y_1) + m_1(Y_1)s + m_2(Y_1)s^2 + m_3(Y_1)s^3 + \cdots. \tag{A2}$$

Now, $m_o(Y_1) = 0$ for an RC tree since for a dc signal (i.e., $s = 0$), $Y_1 = 0$ and $H_1 = 1$. Now, (A1) can be used to obtain the kth moment $m_k(H_1)$ of $H_1(s)$ in terms of the moments of $Y_1(s)$ as follows:

$$\begin{aligned} H_1(s) &= \frac{1}{R_1[m_1(Y_1)s + m_2(Y_1)s^2 + m_3(Y_1)s^3 + \cdots] + 1} \\ &= 1 - R_1 m_1(Y_1)s + \{R_1^2[m_1(Y_1)]^2 - R_1 m_2(Y_1)\}s^2 \\ &\quad + \{2R_1^2 m_1(Y_1)m_2(Y_1) - R_1 m_3(Y_1) \\ &\quad - R_1^3[m_1(Y_1)]^3\}s^3 + \cdots. \end{aligned} \tag{A3}$$

From (A3), the moments $m_0(H_1)$ through $m_3(H_1)$ of the transfer function $H_1(s)$ are a function only of the moments $m_0(Y_1)$ through $m_3(Y_1)$ of the driving point admittance $Y_1(s)$ at node one.

APPENDIX B
CENTRAL MOMENTS FOR AN RC CIRCUIT

For the circuit shown in Fig. 8(b), the central moments $\mu_2^{(1)}$ and $\mu_3^{(1)}$ at node one are related to the moments m_k as follows:

$$\begin{aligned} \mu_2^{(1)} &= 2m_2^{(1)} - [m_1^{(1)}]^2 \\ &= 2[R_1C_1|m_1^{(1)}| + R_1C_2|m_1^{(2)}|] - [m_1^{(1)}]^2 \\ &= 2[R_1C_1(R_1C_1 + R_1C_2) \\ &\quad + R_1C_2(R_1C_1 + R_1C_2 + R_2C_2)] \\ &\quad - (R_1^2C_1^2 + R_1^2C_2^2 + 2R_1^2C_1C_2) \\ &= R_1^2(C_1^2 + C_2^2) + 2R_1^2C_1C_2 + 2R_1R_2C_2^2 \end{aligned} \tag{B1}$$

$$\begin{aligned} \mu_3^{(1)} &= -6m_3^{(1)} + 6m_1^{(1)}m_2^{(1)} - 2[m_1^{(1)}]^3 \\ &= -6[-R_1C_1|m_2^{(1)}| - R_1C_2|m_2^{(2)}] \\ &\quad + 6[m_1^{(1)}][R_1C_1|m_1^{(1)}| + R_1C_2|m_1^{(2)}|] - 2[m_1^{(1)}]^3 \\ &= -6\{-R_1C_1[R_1C_1|m_1^{(1)}| + R_1C_2|m_1^{(2)}|] \\ &\quad - R_1C_2[R_1C_1|m_1^{(1)}| + R_1C_2|m_1^{(2)}| + R_2C_2|m_1^{(2)}|]\} \\ &\quad + 6[m_1^{(1)}][R_1C_1|m_1^{(1)}| + R_1C_2|m_1^{(2)}|] \\ &\quad - 2[m_1^{(1)}]^3 \end{aligned} \tag{B2}$$

where $m_k^{(p)}$ is the kth moment at node p, and

$$\begin{aligned} m_1^{(1)} &= -R_1(C_1 + C_2) \\ m_1^{(2)} &= -R_1(C_1 + C_2) - R_2C_2. \end{aligned} \tag{B3}$$

After some algebraic simplifications, (B3) reduces to

$$\mu_3^{(1)} = 6R_1R_2C_2^2[R_1(C_1+C_2)+R_2C_2]+2[R_1(C_1+C_2)]^3. \tag{B4}$$

When $m_0 = 1$, central moments add under convolution. From (40)

$$\begin{aligned}\mathcal{L}\{\nu_o'(t)\} =& \mathcal{L}\{h(t)\}\cdot\mathcal{L}\{\nu_i'(t)\}\\ =&[m_0(H)+m_1(H)s+m_2(H)s^2+\cdots]\\ &\cdot[m_0(V_i)+m_1(V_i)s+m_2(V_i)s^2+\cdots]\\ =&m_0(H)m_0(V_i)+[m_1(H)m_0(V_i)\\ &+m_0(H)m_1(V_i)]s+[m_2(H)m_0(V_i)\\ &+2m_1(H)m_1(V_i)+m_0(H)m_2(V_i)]s^2+\cdots\end{aligned} \tag{B5}$$

from which the moments of $\mathcal{L}\{\nu_o'(t)\}$ can be obtained as a function of the moments of $H(s)$ and $\mathcal{L}\{\nu_i'(t)\}$. Setting $m_0(V_i)=1$ and $m_0(H)=1$, the central moments of $\mathcal{L}\{\nu_o'(t)\}$ can be simplified to

$$\begin{aligned}\mu_2(V_o) =& 2m_2(H)+2m_2(sV_i)-[m_1(H)]^2-[m_1(sV_i)]^2\\ =&\mu_2(H)+\mu_2(V_i)\\ \mu_3(V_o) =& -6m_3(H)-6m_3(sV_i)+6m_1(H)m_2(H)\\ &+6m_1(V_i)m_2(V_i)-2[m_1(H)]^3-2[m_1(V_i)]^3\\ =&\mu_3(H)+\mu_3(V_i).\end{aligned} \tag{B6}$$

REFERENCES

[1] L. M. Brocco, "Macromodeling CMOS circuits for timing simulation," M.S. thesis, Massachusetts Inst. Technol., Cambridge, June 1987.

[2] P. K. Chan, "An extension of Elmore delay," *IEEE Trans. Circ. Sys.*, vol. CAS-33, no. 11, pp. 1147–1149, Nov. 1986.

[3] C. T. Chen, *Linear System Theory and Design.*, Int. ed. New York: Holt, Rhinehart and Winston, 1984.

[4] C. Chu and M. Horowitz, "Charge-sharing models for switch-level simulation," *IEEE Trans. Computer-Aided Design*, vol. CAD-6, no. 6, pp. 1053–1060, 1987.

[5] H. Cramer, *Mathematical Methods of Statistics.* Princeton, NJ: Princeton Univ. Press, 1946.

[6] F. Dartu, N. Menezes, J. Qian, and L. T. Pillage, "A gate-delay model for high-speed CMOS circuits," in *Proc. 31st Design Automation Conf.*, 1994, pp. 576–580.

[7] W. C. Elmore, "The transient analysis of damped linear networks with particular regard to wideband amplifiers," *J. Appl. Phys.*, vol. 19, no. 1, pp. 55–63, 1948.

[8] W. H. Hayt and J. E. Kemmerly, *Engineering Circuit Analysis.* New York: McGraw-Hill, 1986.

[9] M. A. Horowitz, "Timing models for MOS circuits," Ph.D. thesis, Stanford Univ., Stanford, CA, Jan. 1984.

[10] N. P. Jouppi, "Timing analysis and performance improvement of MOS VLSI designs," *IEEE Trans. Computer-Aided Design*, vol. CAD-6, pp. 650–665, 1987.

[11] M. G. Kendall and A. Stuart, *The Advanced Theory of Statistics, Vol. I: Distribution Theory.* New York: Hafner, 1969.

[12] T.-M. Lin and C. A. Mead, "Signal delay in general RC networks," *IEEE Trans. Computer-Aided Design*, vol. CAD-3, pp. 331–349, 1984.

[13] H. L. MacGillivray, "The mean, median, mode inequality and skewness for a class of densities," *Aust. J. Stat.*, vol. 23, no. 2, pp. 247–250, 1981.

[14] P. R. O'Brien and T. L. Savarino, "Modeling the driving-point characteristic of resistive interconnect for accurate delay estimation," in *Proc. IEEE Int. Conf. Computer-Aided Design*, Nov. 1989, pp. 512–515.

[15] J. K. Ousterhout, "CRYSTAL: A timing analyzer for NMOS VLSI circuits," in *Proc. 3rd Caltech Conf. VLSI*, Mar. 1983.

[16] ——, "Switch-level delay models for digital MOS VLSI," in *Proc. 21st Des. Autom. Conf.*, 1984.

[17] A. Papoulis, *Probability, Random Variables and Stochastic Processes.* New York: McGraw, 1984.

[18] P. Penfield and J. Rubinstein, "Signal delay in RC tree networks," in *Proc. 18th Design Automation Conf.*, 1981, pp. 613–617.

[19] L. T. Pillage and R. A. Rohrer, "Asymptotic waveform evaluation for timing analysis," *IEEE Trans. Computer-Aided Design*, pp. 634–637, Apr. 1990.

[20] E. N. Protonotarios and O. Wing, "Theory of nonuniform RC lines, Part II: Analytic properties in the time domain," *IEEE Trans. Circuit Theory*,pp. 13–20, Mar. 1967.

[21] R. Putatunda, "Auto-delay: A program for automatic calculation of delay in LSI/VLSI chips," in *Proc. 19th Des. Autom. Conf.*, June 1981, pp. 616–621.

[22] C. Ratzlaff and L. T. Pillage, "RICE: Rapid interconnect circuit evaluator using asymptotic waveform evaluation," *IEEE Trans. Computer-Aided Design*, pp. 763–776, June 1994.

[23] J. Rubinstein, P. Penfield, Jr., and M. A. Horowitz, "Signal delay in RC tree networks," *IEEE Trans. Computer-Aided Design*, vol. CAD-2, pp. 202–211, 1983.

[24] C. J. Terman, "Simulation tools for digital LSI design," Ph.D. dissertation, Massachusetts Inst. Technol., Cambridge, MA, Sept. 1983.

[25] M. E. Van Valkenburg, *Introduction to Modern Network Synthesis.* New York: Wiley, 1960.

[26] J. L. Wyatt, *Circuit Analysis, Simulation and Design, Chapter on Signal Propagation Delay in RC Models of Interconnect.* New York: Elsevier, 1987.

Rohini Gupta (S'93–M'95), for a photograph and biography, see this issue, p. 19.

Bogdan Tutuianu was born in Iasi, Romania, on September 15, 1968. He received the Diploma Engineer degree in electronic engineering from the Technical University "Ghe.Asachi," Iasi, Romania, in 1993 and the M.S. degree in electrical and computer engineering from the University of Texas, Austin, in 1995.

Between 1993 and 1994, he held a research position at the Technical University "Ghe.Asachi," Iasi, Romania. He is currently with Motorola Inc., Austin, TX. His research interests include interconnect characterization and analysis.

Lawrence T. Pileggi, formerly Lawrence Pillage, (S'87–M'89–SM'94), for a photograph and biography, see this issue, p. 19.